SURFACE RECOMBINATION IN OXIDE-PASSIVATED SI AFTER THE DEPOSITION OF APCVD TIO2

Andrew F. Thomson*, Keith R. McIntosh*, Bryce S. Richards†
*Center for Sustainable Energy Systems (CSES), † Heriot-Watt University
*Building 32, Australian National University (ANU), ACTON ACT 0200, Australia. Email: andrew.thomson@anu.edu.au,
Phone: +61 261253976, Fax: +61 261250506, †Heriot-Watt University, Edinburgh, EH144AS, U.K

ABSTRACT: Titanium dioxide (TiO_2) is a material with a refractive index well suited for silicon-solar-cell-antireflection coating (ARC). Atmospheric-pressure-chemical-vapor-deposition (APCVD) is a high-throughput inexpensive TiO2-deposition process. Unfortunately TiO_2 affords no passivation to the underlying silicon making TiO_2 films deposited directly on silicon unsuitable for high-efficiency Si solar cells, where low surface recombination is essential. To use TiO_2 as an ARC for high efficiency cells an additional passivating layer is required. In this case a thermal-silicon-oxide (SiO_2) passivating layer is used and the affect of depositing APCVD-TiO_2 on the passivation is investigated.

In this paper we demonstrate that the deposition of APCVD-TiO_2 depassivates the SiO_2—Si interface for planar and textures samples. It was found that for planar samples a post-deposition FGA repairs the depassivation returning the J_{0e} (measured using transient-photoconductance decay) to the pre-deposition value. For textured samples however a post-deposition FGA only part repaired the depassivation of the interface. The non-FGA-repairable depassivation of textured samples a 25-30% increase in J_{0e}. The mechanisms for the depassivation of textured and planar samples were investigated the outcome of the findings are as follows: 1) whilst humidity depassivation was observed in a special case experiment it is immeasurably small when actually depositing TiO_2 films; 2) no depassivation due to contamination was observed in the deposition of TiO_2; 3) hydrogen loss was the sole reason for depassivation in planar samples and responsible for the FGA-repairable depassivation in the textured samples; 4) the cause of the non-FGA-repairable depassivation of textured samples is hypothesised to be stress a related effects of APCVD-TiO_2 deposition.

1 INTRODUCTION

Titanium dioxide is a material that has a refractive index well suited for use in silicon-solar-cell-ARC. The refractive index ranges from 1.9-2.4, largely depends on the temperature of the deposition [1]. APCVD-TiO_2 is deposited using an in-line-belt process, which allows the deposition of inexpensive high throughput ARC. It has been shown by Richards *et. al.* that TiO_2 that can achieve weighted reflectance as low as 8.6% for a single layer ARC and 6.5% for a double layer ARC on planar silicon [2, 3]. If the same ARC was applied to a textured sample this would imply reflectance of less than 1% are possible, if every reflected photon re-strikes the surface at least once [4]. Unfortunately TiO_2 does not passivate the underlying silicon. Good passivation to reduce the surface recombination is necessary to create highly efficient Si solar cells [5]. This paper details our work examining the affect of deposition of APCVD-TiO_2-ARC on the passivation of thermal-SiO_2 passivated silicon. Of particular interest is the effect on the passivation of random-pyramid-textured-oxide-passivated silicon as this is used in a number of high efficiency Si Solar Cells [5, 6], to gain a full understanding of the mechanisms involved both the planar and textured cases were examined.

It was found through this work that deposition of APCVD-TiO_2 has a depassivating effect on the textured and planar Si—SiO_2 interface; this depassivating effect was entirely reversed for the planar samples and only partly reversed for textured samples with a post-deposition forming gas anneal (FGA). The non-FGA reversible depassivaion in the textured samples observed was a 25-30% increase in the emitter saturation current density (J_{0e}). Even with the depassivating effect a J_{0e} of 42.9 fA/cm^2 was achieved on a textured sample, showing this is still a competitive passivating régime [7].

A number of mechanisms have been hypothesised to account for this depassivation. Subsequently both planar and textured samples were processed in the APCVD with varying process parameters to quantify the affect if any of each proposed mechanisms. To understand the origin of the proposed depassivation affects and the experimental process parameters, the basic setup of the SierraTherm 5K6 APCVD is detailed. The APCVD is a 12' long belt furnace, with a CVD injector head in the middle, the injector head sprays a mist of tetra-isopropyl-titanate (TPT) and water vapor on to samples passing on the belt below. Nitrogen gas sheets prevent the reactants mixing until they intercept the top of the passing samples where they mix hydrolysing the TPT creating TiO_2 films [8]. Parameters that can be modified to control the properties of the deposited film are belt speed, reactant / nitrogen carrier ratios, reactant / reactant ratios, total flow rate, and temperature. . Once the system has been calibrated and suitable reactant / reactant ratios have been calculated to control the thickness of the film the belt speed and total gas flow are adjusted. The temperature range of the APCVD can be controlled to between 100 and 500 ^oC, with the effect of changing the crystallographic structure of the TiO_2 film and it optical properties [8].

The proposed depassivation mechanisms are as follows: (1) Hydrogen loss due to the sample being processed at an elevated temperature; the hydrogen-loss reaction (Si_3 = SiH -> Si + H) has an activation energy corresponding to a temperature of ~500 ^oC, the upper processing temperatures possible using the APCVD [9]. (2) Contamination, including metals and organic compounds; the APCVD machine is not in a clean room environment, when processing samples they are simple rested on a metal belt which is heated in the belt furnace ,

there are many possible sources of contamination that might diffused into the samples depassivating the interface and contaminating the bulk. (3) It has been show by L. P. Johnson *et. al.* that the humidity degrades the Si—SiO_2 interface, at 85 ^oC, 85% humidity [10]; water vapor is a reactant at higher temperatures therefore it may be possible that humidity degradation is occurring. (4) Stress effects owing to the deposition of APCVD-TiO_2; due to differing rates of thermal expansion and mismatch between the TiO2-ARC and the underlying substrate, thermal and intrinsic stresses will be generated in the film possibly damaging the underlying passivation [11, 12].

To quantify these possible depassivation mechanisms SiO_2-passivated textured and planar samples were processed in the APCVD, different processing conditions were used to highlight the effect of each mechanism. Through this research it was found that hydrogen loss was observed when processing at 391 ^oC but not 256 ^oC. The loss of hydrogen depassivation could be repaired by a simple Forming Gas Anneal (FGA). No contamination issues arose as a result of any of the experimental processing. Humidity degradation was observed in certain samples but in normal processing situations this degradation appears to be immeasurably small. For planar samples no stress degradation was observed and in fact only reversible loss of hydrogen depassivation of planar samples occurred. Textured samples exhibited depassivation which could not be accounted for entirely by hydrogen loss; we currently attribute to stress related effects and the textured geometry.

2 EXPERIMENTAL METHODOLOGY AND RESULTS

All samples were prepared as follows: 4", 1000 Ω-cm, FZ, <1,0,0>, 300-350 µm, n-type wafers were etched for three minutes in a 1:10 HF:HNO_3 solution. The samples were light $POCl_3$ diffused at 760 ^oC for 20 minutes followed by a deglaze and a 30 minute dry-oxidation at 1100 ^oC and 30 minute in-situ nitrogen anneal at the same temperature. This light diffusion and drive-in oxidation resulted in a diffusion of approximately 200 Ω/□, and oxide thicknesses of 100nm. The same process was followed for the textured samples however the wafer was textured in an IPA-TMAH solution (3.6% TMAH, 12% IPA) prior to the diffusion [13].

To quantify the different degradation mechanisms, the samples were processed in the APCVD using different deposition parameters that are fully detailed below. Some general comments on the results: all J_{0e} measurements were taken with the Ron Sinton photoconductance system using transient decay. For the planar samples the initial J_{0e} measurement was taken from a whole wafer measurement before the wafers were quartered. The textured samples were not measured before the first FGA. All samples were processed on both sides to balance the processing affect, this is necessary for J_{0e} analysis [14]. J_{0e} results calculations were centered at the excess carrier concentration of $1x10^{15}$ $cm^{-3.}$

Table I: Measured J_{0e} (fA/cm^2 per side) for planar and textured samples after processing with no gases to quantify the affect of H-loss and contamination.

Sample	planar-2a		
Iteration	Initial	Post-Process	Post-FGA
Initial	–	8.4	7.6
Run-1	7.6	9.9	7.1
Run-2	7.1	8.0	5.9
Run-3	5.9	7.6	5.6
Sample	planar-2b		
Iteration	Initial	Post-Process	Post-FGA
Initial	–	8.4	6.2
Run-1	6.2	8.9	5.5
Run-2	5.5	7.2	5.1
Run-3	5.1	6.5	5.5
Sample	textured-1		
Iteration	Initial	Post-Process	Post-FGA
Initial	–	–	42.2
Run-1	42.2	55	34.9
Run-2	34.9	47.3	34.3

2.1 Contamination and Hydrogen Loss

To determine the affect of contamination and hydrogen loss the samples were processed at 391 ^oC, with a belt speed of 12"/min, with no process gases. The J_{0e} was measured before and after a post processing 30 minute 400 ^oC FGA, to replace lost hydrogen. The processing of the sample, measurement of J_{0e} and subsequent FGA, were repeated three times to see if there was any cumulative effect of contamination.

The contamination and hydrogen loss results are given in Table I. These results show for planar and textured samples depassivation is occurring after each APCVD process, but this depassivation is repaired after each post-processing FGA. This shows that the depassivation is due to hydrogen being lost during the APCVD processing and the FGA is simply replenishing the lost hydrogen; returning the J_{0e} close to the original value. There is no observed cumulative depassivation effect, indicating that there is negligible contamination occurring during the APCVD process.

Table II: Measured J_{0e} (fA/cm^2 per side) for planar and textured samples after processing with no gases to quantify the affect of H-loss and humidity damage.

Sample	Planar-2c		
Iteration	Initial	Post-Process	Post-FGA
Initial	–	8.4	6.6
run-1	6.6	10.1	7.7
Run-2	7.7	10.9	9.6
Run-3	9.6	11.6	9.8
Sample	Planar-2d		
Iteration	Initial	Post-Process	Post-FGA

Initial	–	8.4	5.9
Run-1	5.9	8.7	7.1
Run-2	7.1	11.8	13.6
Run-3	13.6	10.4	13
Sample	Textured-2		
Iteration	Initial	Post-Process	Post-FGA
Initial	–	–	59.5
Run-1	59.5	64.5	44.5
Run-2	44.5	58.5	55.0
Run-3	55.0	64.0	44.5

2.2 Humidity and Hydrogen Loss

To investigate the effect of humidity depassivation and hydrogen loss the samples were processed at 391 ^{o}C, with a belt speed of 12"/min, with process gas settings of H_2O carrier at 0.8 lpm and H_2O dilutant at 2.2lpm, which is the upper limit on the amount of H_2O processing gases was used. The J_{0e} was measured before and after a post processing FGA, to replace lost hydrogen. This was repeated three times to see if there was any cumulative effect of humidity on the passivation of the samples.

Results for humidity depassivation of planar and textured samples are given in Table **II**. Repetition of this depassivation process show loss and replenishment of hydrogen after subsequent FGA, however the J_{0e} for the planar samples do not return to the initial value. Planar sample 2c shows clear depassivation; the sample never returns to the initial J_{0e} after an FGA. Sample 2d shows depassivation however it J_{0e} is unexpectedly higher after FGA2 this may have been caused by some uncontrolled charging effect. Finally for the textured sample tex-1, no degradation is observed.

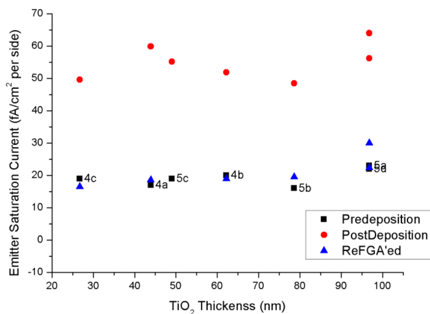

Figure 1: Measured J_{0e} (fA/cm^2 per side) for planar depositing different thickness APCVD-TiO_2films. Each deposition was followed by a FGA to replenish lost hydrogen.

2.3 Stress Effects

Thermal films stress for conformal films is proportional to the difference between deposition temperature and the ambient. For TiO_2 we are unsure how intrinsic film stress will be affected by affected by the temperature and thickness of the deposition. To test different film stress states different temperature and thickness TiO_2 films were deposited. Although thermal film stress is independent of thickness for thick conformal films this may not be the case for thin films as in the sub 100nm TiO_2 films used in this case. For these reasons to investigate the affect film stress has on the passivation of the SiO_2 interface different thickness TiO_2 films were deposited at a 391 ^{o}C and films were also deposited at the same thickness but at 256 and 391 ^{o}C.

Different thickness TiO_2 films were deposited on eight different planar samples; the thickness was altered by changing the overall flow of process gases whilst keeping the H_2O to TPT ratio constant, the process temperature was 391 ^{o}C and the a belt speed 6"/minute. J_{0e} measurements were taken before and after deposition and after a post-deposition FGA the results are depicted in Figure 1, which show that regardless of thickness after a post deposition FGA the J_{0e} return approximately to their original value.

Table III: Measured J_{0e} (fA/cm^2 per side) for planar and textured samples after deposition APCVD TiO_2at different temperatures quantify the affect of stress depassivation. Each deposition was followed by a FGA to replenish lost hydrogen.

Sample	planar-1b		
Dep-Temp	Initial	Post-Process	Post-FGA
256	6.4	6.25	-
Sample	planar-1a		
Dep-Temp	Initial	Post-Process	Post-FGA
391	5.3	8.95	5.65
Sample	textured-1		
Dep-Temp	Initial	Post-Process	Post-FGA
256	34.25	38.75	42.85
Sample	textured-1		
Dep-Temp	Initial	Post-Process	Post-FGA
391	44.5	73.5	59

The cause of the depassivation on textured silicon is not yet fully understood however we have eliminated three possible mechanisms; contamination, humidity and hydrogen loss. It is possible that this depassivation is a stress related affect which will also be the subject of future inquiries. More work will be conducted on the use of thinner more optically realistic films, optimising both for minimal reflectance and the best possible passivation.

The temperature dependence depassivation was tested

for textured and planar samples. Table III depicts the results, the different temperature films were deposited at 256 ^{o}C and 391 ^{o}C, at a belt speed of 8"/min, depositing films ~100nm. J_{0e} measurements were taken before and after a post-deposition FGA. These results show that for planar samples the only apparent degradation is hydrogen loss for the higher temperature deposition; the textured samples however exhibited a depassivation that could not be reversed by a post-deposition FGA.

3 DISCUSSION

In summary, these results show any depassivation exhibited in planar samples after the deposition of APCVD-TiO_2 was reversible with a post-deposition FGA. There was however a measured depassivation for textured samples that could not be reversed with a post-deposition FGA, a 25-30% increase J_{0e} was observed. It was also shown that when samples were repetitively processed with no process gases that there was no permanent depassivation or contamination; the reversible depassivation was attributed to H-loss. Humidity depassivation was observed for planar samples with some inconsistencies more data needs to be taken to make positive assertions about humidity degradation.

For these samples it appears that the temperatures involved in the APCVD process are too low to allow contamination to diffuse into the interface of the samples. These samples however have much thicker SiO_2 passivating layer than what would be used in optically realizable cells, the thicker SiO_2 layer may have acted as a diffusion barrier to contamination. So when thinner layers are used contamination may become a problem, this will be the subject of future inquiries.

Humidity degradation is believed to be the cause of the depassivation of samples 2c and 2d in table Table **II**. To be completely sure of this more results need to be taken. What can be surmised is that humidity degradation when actually depositing a film is non-existent or immeasurably small; this is made apparent in Table III (samples 1a and 1b) where there is no measurable depassivation of the planar samples after deposition of TiO_2. When a film is being deposited the hydrolysation of TPT acts as a sink for the H_2O, preventing it diffusing into the interface degrading the surface passivation. It is assumed that because humidity did not degrade planar sample the cause of the depassivation to the textured samples is not humidity related.

4 REFERENCES

[1] H. J. Hovel, "TiO_2 antireflection coatings by a low temperature spray process," *Elec. Chem. Soc.,* vol. 125, pp. 983-985, 1978.

[2] B. S. Richards, "Comparison of TiO_2 and Other Dielectric Coatings for Buried-contact Solar Cells: a Review," *Prog. Photovolt. Res. Appl.,* vol. 12, pp. 253-281, 2004.

[3] B. S. Richards, "Single material TiO_2 double-layer antireflection coatings," Solar Energy Materials and Solar Cells, 79, 369-390, (2003).

[4] P. Campbell and M. A. Green, "Light trapping properties of pryamidally textured surfaces," *Journal of Appl. Phys.,* vol. 62, p. 7, 1987.

[5] S. W. Glunz, J. Knobloch, C. Hebling, and W. Wettling, " The range of high-efficiency silicon solar cells fabricated at Fraunhofer ISE," in *Photovoltaic Specialists Conference, 1997., Conference Record of the Twenty-Sixth IEEE* Anaheim, CA, USA, 1997.

[6] K. R. McIntosh, N. C. Shaw, and J. E. Cotter, "Light trapping in sunpower's A-300 solar cells," in *Proceedings of 3rd World Conference on: Photovoltaic Energy Conversion, 2003.* Osaka, Japan, 2003.

[7] J. S. M. J. Kerr, A. Cuevas, "Surface recombination velocity of phosphorous-diffused silicon solar cell emitters passivated with plasma enhanced chemical vapor deposited silicon nitride and thermal silicon oxide," *Journal of Applied Physics,* vol. 89, pp. 3821-3826, 1 April 2001 2001.

[8] SierraTherm, "SierraTherm 5k6 manual"

[9] K. L. Brower, "Dissociation kinetics of hydrogen-passivated (111) Si-SiO_2 interface defects," *Physical rev. B,* vol. 42, pp. 3444-3455, 1990.

[10] L. P. Johnson, K. R. McIntosh, B. S. Richards, H. Jin, B. Paudyal, and E. Klampaftis, "Si-SiO_2 Interface Characterisation from Exposure to an Accelerated Humidity Environment,," in *ANZES 2006* ANU, Canberra, Australia: September 2006, 2006.

[11] P. J. Cousins and J. E. Cotter, "Minimizing lifetime degradation associated with thermal oxidation of upright randomly textured silicon surfaces," *Solar Energy Materials and Solar Cells,* vol. 90, pp. 228-240, 24th May 2005 2006.

[12] C. H. Bjorkman, J. T. Fitch, and G. Lucovsky, "Correlation between midga interface state density and thickness-averaged oxide stress and strain at Si/SiO_2 interfaces formed by thermal oxidation of Si," *Appl. Phys. Lett.,* vol. 56, pp. 1983-1985, 1990.

[13] D. Iencinella, E. Centurioni, R. Rizzoli, and F. Zignani, "An optimized texturing process for silicon solar cell substrates using TMAH," *Solar Energy Materials & Solar Cells,* vol. 87 p. 8, 2005.

[14] D. E. Kane and R. M. Swanson, "Measurement of the emitter saturation current by a contactless photoconductivity decay menthod," in *18th IEEE Photovoltaic Specialists Conf*, New York, 1985.